Journal of Engineering Mathematics **26**: 39–50, 1992.
H.K. Kuiken and S.W. Rienstra (eds), Problems in Applied, Industrial and Engineering Mathematics.

Structure of the temperature profile within a high-pressure gas-discharge lamp operating near maximum radiation efficiency

H.K. KUIKEN
Philips Research Laboratories, P.O. Box 80.000, 5600 JA Eindhoven, The Netherlands

Abstract. A singular perturbation technique is used to describe the temperature profile in a wall-stabilized high-pressure gas-discharge arc in the limit of extremely high radiation efficiency. The analysis shows that the profile is characterized by three different regimes, one of which is a transition layer.

Introduction

In this paper we shall investigate a certain aspect of the temperature field produced by a high-pressure gas-discharge arc. The arc is assumed to be enclosed within an elongated cylindrical tube, i.e. it is a so-called wall-stabilized arc. Such a configuration can be technologically important as a high-yield light source. A simplified sketch of such a system is given in Fig. 1.

Two electrodes stick into the tube at both ends. When the lamp is operating, these electrodes are extremely hot, so that they are easily induced to emit electrons. The electric field causes these electrons to accelerate, thereby imparting large amounts of energy to them. The tube is filled with a gas such as mercury or sodium. Because of the high pressure in the tube (from 5 up to 100 atmospheres), the mean free path of the gas molecules is very short, thus collisions with the hot electrons are extremely frequent. During a collision between an electron and a gas molecule the electron loses part of its energy which is transferred to the gas molecule. The electrons soon regain their previous energy levels through the interaction with the electric field.

When a gas molecule absorbs energy as the result of a collision with an electron, the energy transfer may be, roughly speaking, of three different kinds. The energy may be used to increase the temperature of the gas, meaning that it may be returned as translational, vibrational and rotational energy. Indeed, when equilibrium has been reached, the electron temperature and the gas temperature are the same in a high-pressure gas discharge. This is normally known as local thermal equilibrium (LTE). A second energy-transfer mode is the one in which electrons in the outer valence band of the gas molecule are excited to higher quantum levels. Such a higher state may be unstable and, as a result, an excited electron will return to the lower state, possibly through a succession of intermediate states. During this process photons are emitted. As a crude approximation these may be thought to belong to

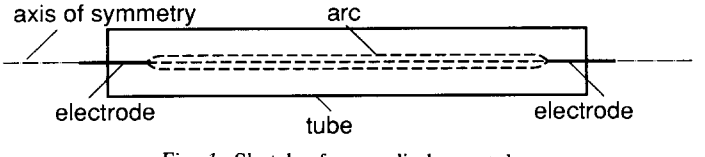

Fig. 1. Sketch of a gas-discharge tube.

two different categories: a) ones that leave the tube without interference; these constitute the lamp's radiation, both visible and invisible; b) ones that are absorbed within the plasma by the gas molecules; this constitutes an added heat-transfer mechanism. The former is called thin radiation and the second is thick radiation. A third electron-gas energy-transfer mode is that in which a gas molecule is ionized. In this process an electron is knocked loose, thereby becoming a free electron.

A knowledge of the temperature field is extremely important for a proper understanding of how a lamp operates. We shall consider the temperature distribution away from the electrodes where it may be thought to depend solely upon the radial coordinate r, assuming stationary conditions. We shall also assume that convection effects are absent, although in larger tubes, particularly in those which are in a vertical position, convection effects may dominate [1, 2, 3]. The one-dimensional rotationally symmetric model we wish to investigate was first described by Elenbaas. A summary of his work can be found in his book on the high-pressure gas discharge [4]. More recent accounts can be found in [5, 6]. Recently, we have shown [7, 8, 9] that this classical model can be treated by asymptotic methods. Since asymptotic methods are capable of giving a much clearer insight into the structure of solutions than could be achieved by any direct computational approach, we decided that the field was worth revisiting.

What we intend to study in this paper is a particular question left open in [9]. It concerns the structure of the temperature field when the maximum radiation efficiency is approached. In that case some important quantities characterizing the arc become singular. It is important to know how.

The model

As explained in [9], the temperature distribution in the middle section of an elongated tube containing a high-pressure gas-discharge arc is governed by the equation

$$\frac{1}{r}\frac{\mathrm{d}}{\mathrm{d}r} r\lambda(t)\frac{\mathrm{d}t}{\mathrm{d}r} + \sigma(t)E^2 - u(t) = 0\,, \tag{1}$$

where t is the temperature, r the distance to the axis symmetry, E the electric field and $\lambda(t)$, $\sigma(t)$ and $u(t)$ the temperature-dependent thermal conductivity, electrical conductivity and radiation output terms, respectively. The electric field E, which is assumed to be uniform, and the total arc current I are related as follows:

$$E = I \Big/ \int_0^a 2\pi r\sigma(t)\,\mathrm{d}r\,, \tag{2}$$

where a is the inner tube radius. The thermal conductivity is assumed to represent ordinary thermal conduction and short-range radiation effects. The latter, which is usually called thick radiation, is to be attributed to photons emitted and absorbed by nearby molecules. It has been shown [9] that the analysis is independent of the particular functional description of $\lambda(t)$. It may even be given in tabulated form.

The electrical conductivity is given by

$$\sigma(t) = \gamma t^{3/4}\exp(-t_i/t)\,, \tag{3}$$

where t_i is equal to half the ionization temperature. If V_i is the ionization potential, i.e. the potential that has to be overcome to dislodge totally an outer electron from the valence band of a gas molecule, then $t_i = eV_i/2k$, where e is the elementary charge and k is Boltzmann's constant. Further, γ is some constant.

Next we have to consider the radiation term $u(t)$ which represents the so-called thin radiation which leaves the tube without hindrance. In [9] we modelled this as follows:

$$u(t) = \omega t^p \exp(-t_*/t) , \tag{4}$$

where the temperature $t_* = eV_*/k$ represents an effective quantized state from which radiation occurs. Since ionization represents the highest energy level attainable, we always have

$$t_* < 2t_i . \tag{5}$$

Further, ω is a constant. The exponent p is usually taken as -1. Boundary conditions are defined as follows:

$$\frac{dt}{dr} = 0 \quad \text{at } r = 0 \text{ (symmetry)} , \tag{6}$$

$$t = t_w \quad \text{at } r = a , \tag{7}$$

where t_w is the (observed) temperature at the inner tube wall.

It has been emphasized before [7, 8, 9] that an effective treatment of a complicated nonlinear system such as the one defined by equations (1–6) can only be done when the system is properly nondimensionalized. Clearly, r can be rendered dimensionless by means of the tube's inner radius a. Arguments were presented in [7, 8, 9] that the temperature is best rendered dimensionless by referring to the axis temperature t_r, which is the maximum temperature in the system. Typical values of t_r are 3000 K–4000 K for sodium arcs and 5000 K–6000 K for mercury arcs. These values are considerably higher than t_w which can be in the range of 1000 K–1500 K, but much lower than either t_i or t_* which are in the range of 50000 K–100000 K. Therefore, neither t_w nor t_i or t_* are suitable reference temperatures. In view of the above, we introduce dimensionless variables as follows:

$$R = r/a , \qquad T = t/t_r . \tag{8}$$

Since t_r is now assumed to have a known value, another parameter has to be turned into an unknown instead. The most natural choice will be the arc current I. By doing this, we invert the problem definition. Instead of asking which maximum temperature t_r results from a given, i.e. observed, arc current, we ask ourselves what arc current is needed to achieve a required axis temperature.

We shall not repeat here the complete derivation of the final equation we wish to investigate. This has already been done in [9], to which we refer for the details. It suffices to note that by means of a Kirchhoff transformation an auxiliary function Q replacing T is defined as follows:

$$Q = T_i \int_T^1 \frac{\lambda(t_r \tilde{T})}{\lambda(t_r)} \, d\tilde{T} , \tag{9}$$

where

$$T_i = \frac{t_i}{t_r} \tag{10}$$

is a large parameter. Because of this, small variations in T result in large variations in Q. As a result, all the interesting phenomena occur in a region where T is close to unity. Asymptotics for $T_i \gg 1$ lead to the following equation for Q:

$$\frac{1}{Z}\frac{\mathrm{d}}{\mathrm{d}Z} Z \frac{\mathrm{d}Q}{\mathrm{d}Z} = \mathrm{e}^{-Q} - \xi\, \mathrm{e}^{-\eta Q}\,, \tag{11}$$

where Z is the stretched radial coordinate

$$Z = R(HT_i)^{1/2}\,. \tag{12}$$

For the definition of H we refer to either [8] or [9]. This parameter is related to the current I and is therefore unknown. It grows exponentially with T_i. It is emphasized that for $Z = O(1)$ the coordinate R is much less than unity. The parameter ξ is related to the radiation efficiency of the arc. It can assume values in the interval

$$0 \leqslant \xi < 1\,. \tag{13}$$

Further, we have

$$\eta = \frac{t_*}{t_i}\,, \tag{14}$$

so that in view of (5) η is always less than 2. In this paper we shall only consider values of η in the interval

$$1 < \eta < 2\,. \tag{15}$$

Boundary conditions at $Z = 0$ are easily obtained from (6) and the requirement that $t = t_r$ at $r = 0$:

$$Q = 0\,, \qquad \frac{\mathrm{d}Q}{\mathrm{d}Z} = 0 \quad \text{at } Z = 0\,. \tag{16}$$

The condition at the inner tube wall now reads

$$Q = T_i \int_{T_w}^{1} \frac{\lambda(t_r T)}{\lambda(t_r)}\,\mathrm{d}T \quad \text{at } Z = (HT_i)^{1/2}\,. \tag{17}$$

We shall not concern ourselves here with condition (17). Its role in the determination of H is one of the main subjects of ref. [9]. Hence, we refer to that paper for the details. Instead, we consider the structure of solutions of the system consisting of equations (11) and (16) for $\xi \uparrow 1$. We shall show that the solution reveals some singular characteristics in that limit. Indeed, if $\xi = 1$, the system admits of the solution $Q \equiv 0$. Numerical solutions for values of ξ close to unity show Q-plots which are not at all as simple as that, or even close to it. These

numerical calculations [9] also indicate that high-performance lamps operate at values of ξ close to unity. This is why a special analysis of the structure of solutions in this range seems warranted.

Asymptotics for $\xi \uparrow 1$ (or $\varepsilon \downarrow 0$)

Let us write

$$\xi = 1 - \varepsilon \tag{18}$$

and consider asymptotics for $\varepsilon \downarrow 0$. Equation (11) now reads

$$\frac{1}{Z}\frac{\mathrm{d}}{\mathrm{d}Z} Z \frac{\mathrm{d}Q}{\mathrm{d}Z} = \mathrm{e}^{-Q} - \mathrm{e}^{-\eta Q} + \varepsilon\, \mathrm{e}^{-\eta Q} . \tag{19}$$

Since $Q \equiv 0$ is a solution for $\varepsilon = 0$, we consider small values of Q first. By introducing

$$Q = \varepsilon P , \tag{20}$$

and expanding the exponential functions for small values of the arguments, we find to first order in ε:

$$\frac{1}{Z}\frac{\mathrm{d}}{\mathrm{d}Z} Z \frac{\mathrm{d}P}{\mathrm{d}Z} - (\eta - 1)P = 1 . \tag{21}$$

Since P must satisfy the conditions imposed upon Q by equation (16), we arrive at

$$Q = \frac{\varepsilon}{\eta - 1} \{I_0((\eta - 1)^{1/2} Z) - 1\} , \tag{22}$$

where I_0 is a modified Bessel function. Since (see Eq. 9.7.1 of [10])

$$I_0(x) \sim \mathrm{e}^x (2\pi x)^{-1/2} \quad \text{for } x \to \infty , \tag{23}$$

we conclude that eventually Q is no longer small. For large values of Z we have

$$Z \sim (\eta - 1)^{-1/2} \{\Omega(\varepsilon) + c_1 + \log(Q)\} , \tag{24}$$

where

$$c_1 = \tfrac{1}{2} \log(2\pi) + \log(\eta - 1) \tag{25}$$

and

$$\Omega(\varepsilon) = \log\left\{ \frac{1}{\varepsilon} \left(\log \frac{1}{\varepsilon} \right)^{1/2} \right\} . \tag{26}$$

Clearly, the function Q becomes of order unity when $Z - (\eta - 1)^{-1/2} \Omega(\varepsilon)$ is of order

unity. To describe the function Q in this region we introduce the translated coordinate z as follows:

$$Z = (\eta - 1)^{-1/2}\Omega + z\,, \tag{27}$$

where z is $O(1)$ in the limit $\varepsilon\downarrow 0$. Since Q is now assumed to be of order unity, no further scaling is necessary. Introducing (27) in (19), assuming that Q and its derivatives with respect to z are all of order unity, we obtain the equation

$$\frac{\mathrm{d}^2 Q}{\mathrm{d}z^2} = \mathrm{e}^{-Q} - \mathrm{e}^{-\eta Q}\,. \tag{28}$$

The solution to this equation must match with the previous one in accordance with the rule (24) for $z \to \infty$, i.e.

$$z \sim (\eta - 1)^{-1/2}\{c_1 + \log(Q)\} \quad \text{for } z \to -\infty \quad (Q\downarrow 0)\,. \tag{29}$$

On integrating equation (28) once, we obtain

$$\frac{1}{2}\left(\frac{\mathrm{d}z}{\mathrm{d}Q}\right)^{-2} = \text{constant} - \mathrm{e}^{-Q} + \frac{1}{\eta}\,\mathrm{e}^{-\eta Q}\,. \tag{30}$$

If the solution to this differential equation is to behave in accordance with the matching condition (29), the constant must be equal to $1 - \eta^{-1}$. Integrating once more, we find

$$z = c_2 + 2^{-1/2}\int_1^Q \frac{\mathrm{d}q}{\{1 - \mathrm{e}^{-q} - (1 - \mathrm{e}^{-\eta q})/\eta\}^{1/2}}\,, \tag{31}$$

where c_2 is a constant of integration. It can easily be shown that the behaviour of (31) for $Q\downarrow 0$ is

$$z \sim c_2 + c_3 + (\eta - 1)^{-1/2}\log(Q)\,, \tag{32}$$

where

$$c_3 = \int_0^1 \left\{\frac{1}{(\eta - 1)^{1/2}Q} - \frac{1}{2^{1/2}\{1 - \mathrm{e}^{-Q} - (1 - \mathrm{e}^{-\eta Q})/\eta\}^{1/2}}\right\}\mathrm{d}Q\,. \tag{33}$$

By comparing (29) and (32), we conclude that the integration constant c_2 is given by

$$c_2 = c_1(\eta - 1)^{-1/2} - c_3\,. \tag{34}$$

On the other hand, the behaviour of equation (31) for $z \gg 1$ is given by

$$z \sim c_2 + c_4 + \left\{\frac{\eta}{2(\eta - 1)}\right\}^{1/2} Q\,, \qquad (Q \to \infty)\,, \tag{35}$$

where

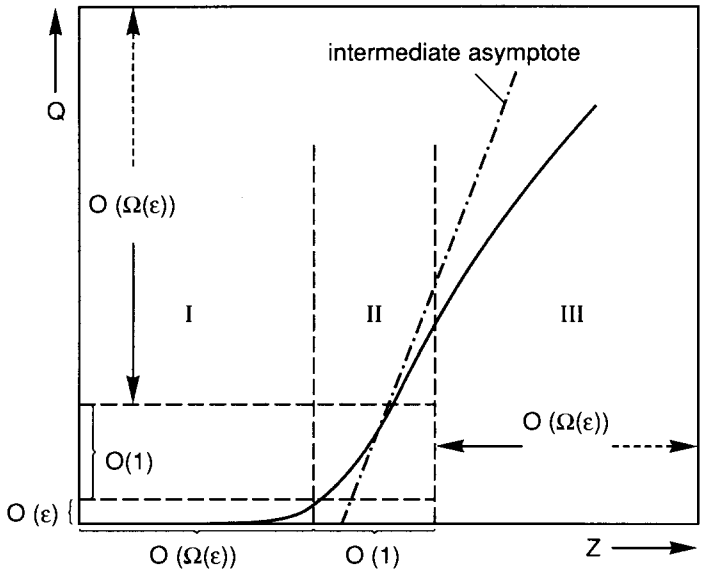

Fig. 2. Schematic picture of the three-layer structure of the temperature field.

$$c_4 = 2^{-1/2}\int_1^{\infty}\left\{\frac{1}{\{1-e^{-Q}-(1-e^{-\eta Q})/\eta\}^{1/2}}-\left(\frac{\eta}{\eta-1}\right)^{1/2}\right\}dQ-\left(\frac{\eta}{2(\eta-1)}\right)^{1/2}. \tag{36}$$

Apparently, this solution approaches an oblique asymptote with an intercept on the Z-axis at $z = c_2 + c_4$ or, using (27), at

$$Z = Z_0 = (\eta-1)^{-1/2}\Omega(\varepsilon) + c_2 + c_4 \tag{37}$$

and a slope equal to $\{\eta/2(\eta-1)\}^{1/2}$.

In Fig. 2 we present a schematic picture of the two regions which emerged from the analysis so far. First we have region I in which Q remains $O(\varepsilon)$. The Z-range, in which this part of the solution defined by (22) is valid, extends up to distances from the origin which are $O(\Omega(\varepsilon))$. This is followed by a region II in which Q and its derivatives rise rapidly to values that are of order unity. The width of this region is of order unity. This part of the solution is defined by equations (27) and (31). The differential equation which governs the solution in region II is given by equation (28). From this equation the term $Z^{-1}\,dQ/dZ$ is absent. Indeed, with Q and its derivatives being of order unity here, the term Z^{-1} renders this particular term $O(\Omega^{-1})$. We shall see later that this term regains first-order importance in a third region in which both Z and Q are allowed to tend to infinity.

Region III

The solution we found in region II, the transition region, applies as long as z is much smaller than $\Omega(\varepsilon)$. Suppose $z = \delta\Omega(\varepsilon)$, where δ is a small but fixed parameter $(0 < \delta \ll 1)$. Letting $\varepsilon\downarrow 0$, we conclude that the solution in region II is given approximately by the asymptote of equation (35). The term $Z^{-1}\,dQ/dZ$ is still of the order of Ω^{-1} and the term $\exp(-Q)$ is of the order $\exp(-\tau\Omega)$, where τ is some constant larger than zero and independent of ε.

Therefore, as soon as we are well into the tail of the solution in region II, the exponentials are negligibly small in comparison with the other terms in the equation. This leads to the conclusion that the solution in region III is governed by the differential equation

$$\frac{d^2Q}{dZ^2} + \frac{1}{Z}\frac{dQ}{dZ} = 0 . \tag{38}$$

The solution must approach the asymptote (35) from the other side, i.e.

$$Q = 0 , \quad \frac{dQ}{dZ} = \left(\frac{2(\eta - 1)}{\eta}\right)^{1/2} \quad \text{at } Z = Z_0 . \tag{39}$$

The solution to this problem is

$$Q = \left(\frac{2(\eta - 1)}{\eta}\right)^{1/2} Z_0 \log(Z/Z_0) . \tag{40}$$

This expression shows that in the outer region Z_0 is the natural scaling factor for both Q and Z. (See also Fig. 2.)

Composite solutions

We can define composite solutions on the basis of the partial solutions that are valid in regions I, II and III, respectively. Because of the way in which the solution is given in region II, we shall define composite solutions with Q as the independent variable. The common (matched) part of the solutions in regions I and II is

$$\mathrm{CP(I, II)} = (\eta - 1)^{-1/2}\Omega(\varepsilon) + c_2 + c_3 + (\eta - 1)^{-1/2} \log(Q) . \tag{41}$$

This follows from (27) and (32). Therefore, the composite solution which comprises the regions I and II is

$$Z_{\mathrm{comp}}(\mathrm{I, II}) = (\eta - 1)^{-1/2} \,\mathrm{inv}\, I_0(Q(\eta - 1)/\varepsilon) + Z_{\mathrm{II}} - \mathrm{CP(I, II)} , \tag{42}$$

where inv I_0 denotes the inverse Bessel function I_0. Further, Z_{II} is defined by (27) and (31). This solution applies in the interval

$$0 \leqslant Z \leqslant (1 + \delta)Z_0 , \tag{43}$$

where δ is a small, but fixed, positive constant ($0 < \delta \ll 1$).

When Q is of the order of ε, the inv I_0 function represents a non-trivial contribution to (42). It can easily be shown that Z_{II} is then approximately equal to the common part. On the other hand, when Q becomes much larger than ε, the common part cancels approximately the first term on the right of (42). The latter result will be used in a later section.

It is also possible to make a composite solution on the basis of the solutions that are valid in the regions II and III. The part these two solutions have in common is defined by (27) and (35). Therefore,

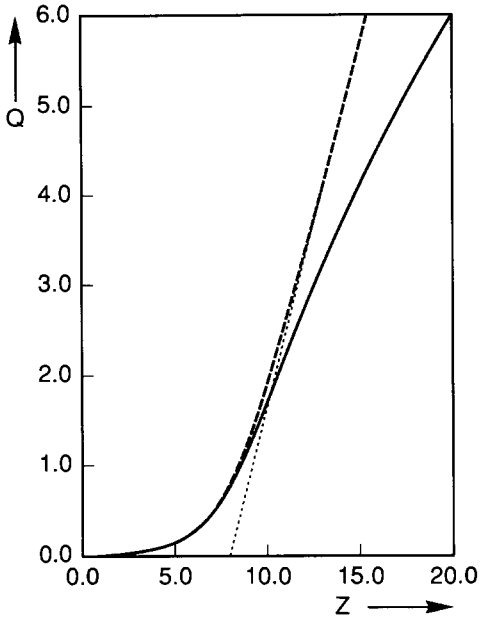

Fig. 3.

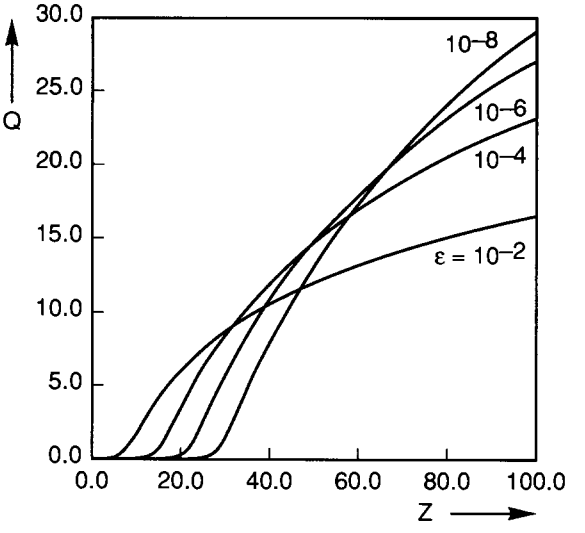

Fig. 4.

Fig. 3. $Z_{\text{comp}}(\text{I, II})$ given by dashed curve and $Z_{\text{comp}}(\text{II, III})$ given by fully drawn curve for $\varepsilon = 0.01$ and $\eta = 1.5$. The dotted line represents the intermediate asymptote.

Fig. 4. The temperature function Q for four different values of ε. ($\eta = 1.5$)

$$Z_{\text{comp}}(\text{II, III}) = Z_{\text{II}} + Z_0 \exp\left\{\left(\frac{\eta}{(2\eta - 1)}\right)^{1/2} \frac{Q}{Z_0}\right\} - Z_0 - \left(\frac{\eta}{(2\eta - 1)}\right)^{1/2} Q\,, \tag{44}$$

where Z_{II} is defined by the sum of equations (27) and (31). This composite solution applies in the regions II and III. This renders it at once more practical than equation (42). Indeed, since the values of Q in region I are only $O(\varepsilon)$, the overall picture of the temperature profile is well represented by (44). A graph showing the two composite expansions is presented in Fig. 3, together with the intermediate asymptote.

Figure 4 shows temperature profiles for various values of ε and $\eta = 1.5$. These profiles indicate that the transition layer moves further and further away from the origin, as ε becomes smaller and smaller. The changeover from region I to region III seems to become more and more rapid. It is also interesting to note that two different profiles have a point in common outside the origin. The envelope of the family of curves can easily be calculated from Eq. (40), namely by varying the parameter Z_0. This envelope is the straight line $Q = (2(\eta - 1)/\eta)^{1/2}\, \mathrm{e}^{-1} Z$.

Characteristic functions

In the analysis of reference [9] two functions $g_1(\xi, \eta)$ and $g_2(\xi, \eta)$ are of particular importance. They are defined by the asymptotic behaviour of Q for $Z \to \infty$:

$$Q \to g_1(\xi, \eta) \log(Z) - g_2(\xi, \eta)\,. \tag{45}$$

From the analysis of this paper we conclude the following (see equations (40), (37) and (18)):

$$g_1(\xi, \eta) = (2/\eta)^{1/2}\{\Omega(1-\xi) + O(1)\}\,, \tag{46}$$

$$g_2(\xi, \eta) = g_1(\xi, \eta)\log\{(\eta-1)^{-1/2}\Omega(1-\xi) + O(1)\} \tag{47}$$

for $\xi\uparrow 1$. Another useful quantity defined in [9] is the lamp's efficiency:

$$W = \xi \int_0^\infty Z\,\mathrm{e}^{-\eta Q}\,\mathrm{d}Z \Big/ \int_0^\infty Z\,\mathrm{e}^{-Q}\,\mathrm{d}Z\,. \tag{48}$$

To be able to calculate this function we must evaluate asymptotically the integral

$$I(\nu) = 2\int_0^\infty Z\,\mathrm{e}^{-\nu Q(Z)}\,\mathrm{d}Z\,. \tag{49}$$

Since Q is a monotonically increasing function of Z we obtain from integration by parts:

$$I(\nu) = \tfrac{1}{2}\nu \int_0^\infty Z^2\,\mathrm{e}^{-\nu Q}\,\mathrm{d}Q\,. \tag{50}$$

In view of the availability of the two composite solutions (42) and (44), we shall write

$$I(\nu) = \tfrac{1}{2}\nu \int_0^{Q_0} Z^2_{\mathrm{comp}}(\mathrm{I},\mathrm{II})\,\mathrm{e}^{-\nu Q}\,\mathrm{d}Q + \tfrac{1}{2}\nu \int_{Q_0}^\infty Z^2_{\mathrm{comp}}(\mathrm{II},\mathrm{III})\,\mathrm{e}^{-\nu Q}\,\mathrm{d}Q\,, \tag{51}$$

where

$$Q_0 = Q((1+\delta)Z_0)\,, \tag{52}$$

with $0 < \delta \ll 1$ fixed. It can easily be seen that Q_0 is well within the asymptotic range defined by (35). Therefore, the upper bound of the first integral of (51) can be replaced by ∞. The very first part of the integration range, where Q is of the order of ε, can be disregarded, since its contribution to the integral is asymptotically zero, namely $O(\varepsilon)$, with respect to the terms retained. Therefore, the first integral reads approximately

$$\tfrac{1}{2}\nu \int_0^\infty Z^2_{\mathrm{II}}\,\mathrm{e}^{-\nu Q}\,\mathrm{d}Q \sim \frac{\Omega^2(\varepsilon)}{2(\eta-1)} + \frac{\Omega(\varepsilon)}{(\eta-1)^{1/2}}\left\{c_2 + 2^{-1/2}\int_1^\infty \frac{\mathrm{e}^{-\nu Q}\,\mathrm{d}Q}{\{1-\mathrm{e}^{-Q}-(1-\mathrm{e}^{-\eta Q})/\eta\}^{1/2}}\right.$$
$$\left. - 2^{-1/2}\int_0^1 \frac{(1-\mathrm{e}^{-\nu Q})\,\mathrm{d}Q}{\{1-\mathrm{e}^{-Q}-(1-\mathrm{e}^{-\eta Q})/\eta\}^{1/2}}\right\} + o(\Omega)\,. \tag{53}$$

The second integral of (51) can be shown to be asymptotically smaller than any of the terms retained in (53). Equation (48) can now be evaluated for $\xi\uparrow 1$, i.e. for $\varepsilon\downarrow 0$. After some manipulations we find

$$W \sim 1 - 2^{3/2}(\eta-1)\eta^{-1/2}\Omega^{-1}(\varepsilon) + o(\Omega^{-1})\,, \tag{54}$$

showing that the radiation-efficiency parameter tends to unity when $\xi\uparrow 1$ or $\varepsilon\downarrow 0$.

In [9] we derived

$$g_1(\xi,\eta)=\int_0^\infty Z(\mathrm{e}^{-Q}-\xi\,\mathrm{e}^{-\eta Q})\,\mathrm{d}Z=I(1)-I(\eta)\,. \tag{55}$$

Using the result of Eq. (53), we find for $\xi\uparrow 1$

$$\begin{aligned} g_1(\xi,\eta)&\sim 2^{-1/2}(\eta-1)^{-1/2}\Omega(1-\xi)\int_0^\infty \frac{\mathrm{e}^{-Q}-\mathrm{e}^{-\eta Q}}{\{1-\mathrm{e}^{-Q}-(1-\mathrm{e}^{-\eta Q})/\eta\}^{1/2}}\,\mathrm{d}Q \\ &=2^{1/2}\eta^{-1/2}\Omega(1-\xi)\,. \end{aligned} \tag{56}$$

By comparing this with (46), we conclude that the leading-order terms match. This may serve as a useful check on the correctness of the present analysis.

Concluding remarks

In this paper we have described the asymptotic form of the temperature profile in a wall-stabilized high-pressure gas-discharge arc, when the radiation-efficiency parameter approaches unity. This case applies when the heat-input term and the radiation-loss term become almost equally important. In this limit the temperature remains virtually constant ($t\sim t_r$) in a central portion of the arc. This is followed by a thin transition region in which the temperature profile rapidly bends downwards. Both the heat-input term and the radiation-loss term play a first-order role in these two regions. Next to the transition region, away from the axis, the temperature profile follows a simple logarithmic rule. In this region, which extends all the way to the inner tube wall, neither the energy source nor the loss term play a first-order role. For the practical implementation of the results of this paper and for a more complete discussion of these, we refer to the companion paper [9].

In this communication we have limited ourselves to presenting the leading-order terms of the three expansion solutions. Clearly, these suffice for bringing out the structure of the temperature profile. It would seem to be possible to derive a few more terms in each of the expansions. However, we postpone that to a future paper [11]. To illustrate that, apart from bringing forth the structure of the asymptotic temperature profiles, the leading terms of the asymptotic expansions are also capable of giving useful numerical results, we present Table 1. This table gives asymptotic and numerically evaluated values of the radiation-efficiency

Table 1. Radiation efficiency W for various values of ε and for $\eta=1.5$

$\log_{10}(\varepsilon)$	Equation (54)	Exact (numerical)
−1	0.575	0.594
−2	0.785	0.768
−3	0.853	0.842
−4	0.888	0.880
−5	0.9093	0.9036
−6	0.9237	0.9194
−7	0.9341	0.9308
−8	0.9419	0.9393
−9	0.9481	0.9460
−10	0.9531	0.9513

parameter W. The numerical values were obtained with the software discussed in ref [9]. Clearly, even for $\varepsilon = 0.1$ or $\xi = 0.9$ the asymptotic result is quite useful. It is interesting to note that ε must become extremely small for W to approach the limiting value of unity. Since radiation efficiencies larger than 0.5 are not uncommon for many lamps, the asymptotic treatment would seem to be quite useful.

To conclude, we remark that the problem area studied here shows great similarities with certain fields in combustion theory. Expressions such as (3) or (4), with rapidly varying exponential terms, are also characteristic of problems dealing with thermal explosions. Singular perturbation techniques are frequently needed to describe the solutions of such problems adequately. We refer to [12, 13] for further details. What seems to distinguish our problem from combustion problems is that we have to deal with two competing exponential functions, as shown by equation (11). In this paper we studied what happens when this competition is at its extreme.

References

1. R.J. Zollweg, Convection in vertical high-pressure mercury arcs. *J. Appl. Phys.* 49 (1978) 1077–1091.
2. J.J. Lowke, Calculated properties of vertical arcs stabilized by natural convection. *J. Appl. Phys.* 50 (1979) 147–157.
3. H.K. Kuiken, A boundary-layer model for a plane free-burning high-pressure gas-discharge arc. *J. Appl. Phys.* 69 (1991) 2896–2903.
4. W. Elenbaas, *The High Pressure Mercury Vapour Discharge*. Amsterdam: North Holland Publishers (1951) 173 pp.
5. J.F. Waymouth, *Electric Discharge Lamps*. Cambridge: M.I.T. Press (1971) 353 pp.
6. J.J. de Groot and J.A.J.M. van Vliet, *The High-Pressure Sodium Lamp*. Deventer: Kluwer Technische Boeken B.V. (1986) 328 pp.
7. H.K. Kuiken, Thermal behaviour of a high-pressure gas-discharge lamp. To appear in: Lecture Notes in Mathematics, *Mathematical Modelling of Industrial Processes*. Heidelberg: Springer (1991).
8. H.K. Kuiken, An asymptotic treatment of the Elenbaas–Heller equation. *Appl. Phys. Letters* 58 (1991) 1833–1835.
9. H.K. Kuiken, An asymptotic treatment of the Elenbaas–Heller equation for a radiating wall-stabilized high-pressure gas-discharge arc. *J. Appl. Phys.* 70 (1991) 5282–5291.
10. M. Abramowitz and I.A. Stegun, *Handbook of Mathematical Functions*. Seventh Edition. Washington: Nat'l Bur. Stands. (1968) 1046 pp.
11. H.K. Kuiken, Higher approximations to the solution of a problem concerning a high-pressure gas-discharge arc. To appear in *Appl. Math. Letters*, 1992.
12. J.D. Buckmaster and G.S.S. Ludford, *Theory of Laminar Flames*. Cambridge: Cambridge University Press (1982) 266 pp.
13. A. Kapila, *Asymptotic Treatment of Chemically Reacting Systems*. Boston: Pitman (1983) 119 pp.